

Mulberry Extract Inhibits Ferroptosis Through Antioxidant Activity, Iron Chelation, and Multi-Target Regulation: Insights from in Vitro and in Silico Study

Kaidi Song¹, Meng Li¹, Zhenlin Wei^{2,*}

¹ School of Life Sciences, Dezhou University, Dezhou Shandong, 253000, China

² Institute for Rural Revitalization, Dezhou University, Dezhou Shandong, 253000, China

* Corresponding author: Zhenlin Wei (Email: wzl19741028@163.com)

Abstract

Ferroptosis is a novel modifiable mode of cell death. Mulberry extract has antioxidant capacity, a hepatoprotective effect, and the ability to alleviate carbon tetrachloride-induced liver injury. However, whether it can complex iron ions and inhibit the activity of the key enzyme of Ferroptosis has not yet been reported. In this study, we used virtual screening, molecular docking, and molecular dynamics analysis to elucidate the anti-Ferroptosis components and mechanism of action in mulberry.

Keywords

Mulberry Extract; Ferroptosis; Glutathione; Molecular Docking.

1. Introduction

Mulberry (*Fructus Mori*), the ripe fruit of plants from the Moraceae family. It was officially listed as a "medicinal and food" agricultural product by the Ministry of Health of China in 1993[1]. However, its potential to chelate iron ions and inhibit key processes in ferroptosis remains unexplored, presenting a significant knowledge gap.

Ferroptosis is a recently identified form of regulated cell death (RCD) characterized by dysregulated iron metabolism, accumulation of reactive oxygen species (ROS), and lethal lipid peroxidation[2,3]. Given the central role of iron and oxidative stress in ferroptosis, we hypothesized that the antioxidant-rich mulberry extract might also function as an iron chelator and ferroptosis inhibitor.

The pivotal trigger for the lipid peroxidation cascade in ferroptosis is the aberrant accumulation of redox-active Fe^{2+} , which fuels the Fenton reaction to generate cytotoxic ROS[4]. Among PUFA, arachidonic acid (AA) and adrenic acid (AdA) are particularly susceptible to oxidation. In the enzymatic lipid peroxidation pathway, acyl-CoA synthetase long-chain family member 4 (ACSL4) catalyzes the conversion of AA/AdA to their CoA esters, which are then incorporated into membrane phospholipids via lysophosphatidylcholine acyltransferase 3 (LPCAT3) to form AA/AdA-phosphatidylethanolamine (AA/AdA-PE). Finally, lipoxygenases (LOXs) oxidize AA/AdA-PE to generate PE-AA/AdA-OOH, a key mediator of ferroptosis [5,6].

Cellular defense against ferroptosis primarily relies on systems that eliminate lipid peroxides. Recently, parallel pathways—such as FSPI/CoQ10/NAD(P)H, DHODH/CoQH₂, GCH1/BH₄, and iNOS—have been identified as suppressors of ferroptosis through their anti-peroxidative functions.

Iron overload and oxidative stress are recognized as major drivers of liver injury and disease progression in numerous hepatic disorders [7]. Notably, the iron chelator deferoxamine and the specific ferroptosis inhibitor Ferrostatin-1 (Fer-1) can reverse these ferroptotic features and mitigate hepatotoxicity [8].

The global burden of liver disease is substantial, responsible for approximately 2 million deaths per year and accounting for 4% of global mortality. However, the development of drugs specifically targeting ferroptosis is still in its infancy, underscoring the urgent need to explore novel and effective modulators.

In this study, we systematically analyzed the capacity of mulberry extract and its constituents to inhibit ferroptosis. Ultimately, our research establishes an experimental foundation for developing mulberry-derived nutraceuticals aimed at preventing liver injury by targeting ferroptosis.

2. Experimental Materials and Methods

2.1. Materials and Reagents

Erastin, ferrostatin-1, GSH/GSSG kit, and MTT kit were purchased from Biyuntian Biotechnology Company. The rest of the biochemical reagents were purchased from Shanghai Sangong Bioengineering Company Limited. Dried mulberry was purchased from the market of Xajing County. HeLa cells were preserved in this laboratory.

2.2. Mulberry Extract Preparation and Property Analysis

2.2.1. Mulberry Extract Preparation

Dried mulberries were washed three times with purified water and subsequently dried. The material was ground into a fine powder. 10 g of the powder was mixed with 100 mL of purified water and extracted by sonication for 20 minutes. The extract was then centrifuged at 10,000 rpm for 10 minutes, and the supernatant was filtered through a 0.45 μm membrane to remove insoluble substances. The filtered solution was lyophilized for 2–3 days to obtain a freeze-dried powder. This powder was dissolved in purified water, sterilized by filtration through a 0.22 μm membrane, and stored as mulberry extract at 4°C for subsequent use [9].

2.2.2. Determination of Antioxidant Capacity of Mulberry Extracts

The antioxidant capacity of the mulberry extract was evaluated using ABTS (2,2'-azino-bis(3-ethylbenzothiazoline-6-sulfonic acid) diammonium salt) and DPPH (1,1-diphenyl-2-picrylhydrazyl) radical scavenging assays.

In the ABTS assay, the ABTS reagent was dissolved in ultrapure water and kept in the dark for 12–16 hours to form the radical cation, which was adjusted to an absorbance of 0.7 at 734 nm. Then, 188 μL of the ABTS working solution was mixed with 12 μL of the mulberry extract at different concentrations. The mixture was transferred to a 96-well plate, incubated at room temperature for 30 minutes, and the absorbance at 734 nm was measured using a microplate reader. Ascorbic acid was used as a positive control [10].

For the DPPH assay, DPPH was dissolved in anhydrous ethanol, and the solution was adjusted to an absorbance of 1.2 at 520 nm. Next, 150 μL of the DPPH working solution was mixed with 50 μL of the mulberry extract at different concentrations. After incubation in the dark for 30 minutes, the absorbance at 520 nm was measured using a microplate reader. Ascorbic acid served as the control [11].

The calculation formula for this is as follows:

$$\text{clearance rate} = (A_{\text{control}} - A_{\text{treat}}) / A_{\text{control}} \times 100\%$$

2.2.3. Determination of Fe²⁺ and Fe³⁺ Ion Chelating Capacity

The iron chelating activity of the mulberry extract was evaluated using established methods with modifications.

For the Fe²⁺ chelating assay, 50 μL of the mulberry extract at varying concentrations was mixed with 50 μL of FeSO₄ solution (50 μM) in a 96-well plate. After incubation at room temperature

for 10 min, 100 μL of ferrozine solution (0.5 mM) was added. The mixture was shaken thoroughly and allowed to stand for another 10 min. The absorbance was then measured at 562 nm using a spectrophotometer. A blank control (100 μL PBS + 100 μL ferrozine) and negative controls (50 μL PBS + 50 μL extract + 100 μL ferrozine; 50 μL PBS + 50 μL FeSO_4 + 100 μL ferrozine) were included [12,13].

For the Fe^{3+} chelating assay, 50 μL of the mulberry extract was mixed with 50 μL of FeCl_3 solution (0–100 μM). Subsequently, 50 μL of FeSO_4 solution (50 μM) was added, and the mixture was stirred thoroughly. Following a 10-min incubation at room temperature, 100 μL of potassium thiocyanate (KSCN) color developer was added. After mixing and reacting for 5 min, the reddish $\text{Fe}(\text{SCN})_3$ complex formed, and its absorbance was measured at 470 nm. Control groups included a blank (100 μL PBS + 100 μL KSCN), a negative control (50 μL PBS + 50 μL extract + 100 μL KSCN), and a final control (50 μL PBS + 50 μL FeCl_3 + 100 μL KSCN) [14].

The calculation formulae for the two groups are as follows:

$$\text{chelating ratio (\%)} = \left(1 - \frac{A_{\text{treat}} - A_{\text{blank}}}{A_{\text{negative}} - A_{\text{blank}}}\right) * 100$$

2.3. Analysis of the Inhibitory Effect of Mulberry Extract on Cell Ferroptosis

2.3.1. Cytotoxicity Assessment of Mulberry Extract via MTT Assay

HeLa cells were maintained in DMEM (Gibco) supplemented with 10% fetal bovine serum (FBS, Gibco) and 1% penicillin/streptomycin (HyClone) at 37°C in a 5% CO_2 atmosphere. Cells in the logarithmic growth phase were harvested by digestion with 0.25% trypsin (Sigma), resuspended, and seeded into 96-well plates (Corning) at a density of 5×10^3 cells per well. After 24 h of incubation, the cells were treated with mulberry extract (0–1600 $\mu\text{g}/\text{mL}$, sterilized by 0.22 μm filtration) or Erastin (0.25–10 μM , MedChemExpress) for another 24 h, with a blank control group included.

Subsequently, 20 μL of MTT solution (5 mg/mL, Sigma) was added to each well and incubated for 4 h. The supernatant was then carefully removed, and 100 μL of DMSO (Sigma) was added to dissolve the formazan crystals. The absorbance at 570 nm was measured using a microplate reader (BioTek Synergy H1), and cell viability was calculated as follows:

$$\text{survival ratio (\%)} = \frac{A_{\text{treat}} - A_{\text{blank}}}{A_{\text{control}} - A_{\text{blank}}} * 100\%$$

2.3.2. Mitigation of Erastin-induced Ferroptosis by Mulberry Extract

HeLa cells in the logarithmic growth phase were trypsinized, resuspended in complete DMEM with 10% FBS. The cell suspension was seeded into 96-well plates at 5×10^3 cells per well and incubated for 24 h to allow attachment. Cells were pretreated for 1 h with three preselected concentrations of mulberry extract (filter-sterilized) or Ferrostatin-1 (Fer-1, Sigma), followed by the addition of gradient concentrations of Erastin and further incubation for 24 h.

After treatment, the MTT assay was performed as described in Section 2.4.1. Briefly, 100 μL of culture medium was aspirated, 20 μL of MTT solution (5 mg/mL) was added per well, and plates were incubated for 4 h. The formed formazan crystals were dissolved in 100 μL DMSO with gentle shaking at 37°C until fully solubilized. Absorbance at 570 nm was measured using a microplate reader (BioTek Synergy H1), and cell viability was calculated accordingly.

2.4. Analysis of the Mechanism of Inhibition of Cellular Iron Death by Mulberry Extracts

2.4.1. Analysis of Intracellular Reduced Glutathione (GSH) Content

Cell culture and treatment: HeLa cells were seeded into 6-well plates (Corning) and cultured until they reached 70–80% confluence. Following a 6-hour drug treatment according to the experimental design, the cells were washed twice with PBS (HyClone), detached using 0.25% trypsin (Sigma), and collected by centrifugation at 1000 rpm for 5 min. The supernatant was carefully discarded.

GSH extraction: The cell pellet was resuspended in three volumes of Protein Removal Reagent M (Beyotime) and vortexed thoroughly. The mixture was subjected to two freeze-thaw cycles. The lysate was then centrifuged at 10,000 rpm for 10 min at 4°C (Eppendorf 5424R). The resulting supernatant was collected and diluted 15-fold with PBS to obtain the test sample.

GSH quantification: GSH standards (Sigma) or prepared samples were added in sequence to a 96-well plate (Corning). Then, 150 μ L of the total glutathione assay working solution (Beyotime) was added to each well. After mixing and incubating at room temperature for 5 min, 50 μ L of NADPH solution (0.5 mg/mL, Sigma) was added and mixed immediately. The absorbance at 412 nm was dynamically monitored using a microplate reader (BioTek Synergy H1) over a period of 25 min, with measurements taken at 5-min intervals [15].

2.4.2. Molecular Docking Analysis

Molecular docking was performed to evaluate the interactions between bioactive compounds derived from mulberry and key proteins involved in ferroptosis. The binding pockets for each protein were predicted using CB-Dock2 software. Molecular docking simulations were carried out with AutoDock Vina, and the resulting binding poses were validated using AMDock [16].

The pharmacokinetic properties of the candidate compounds were predicted using the ADMETlab 3.0 platform (<https://admetlab3.scbdd.com>). All ligand structures were uniformly converted into SMILES format prior to analysis [17].

2.5. Statistical Analyses

All statistical analyses were performed using GraphPad Prism software (version 9.5). Data are presented as the mean \pm standard deviation (SD). Differences among treatment groups were assessed by one-way analysis of variance (ANOVA), followed by an appropriate post-hoc test for multiple comparisons. A p-value of less than 0.05 was considered statistically significant.

3. Results and Discussion

3.1. Antioxidant Capacity of Mulberry Extracts

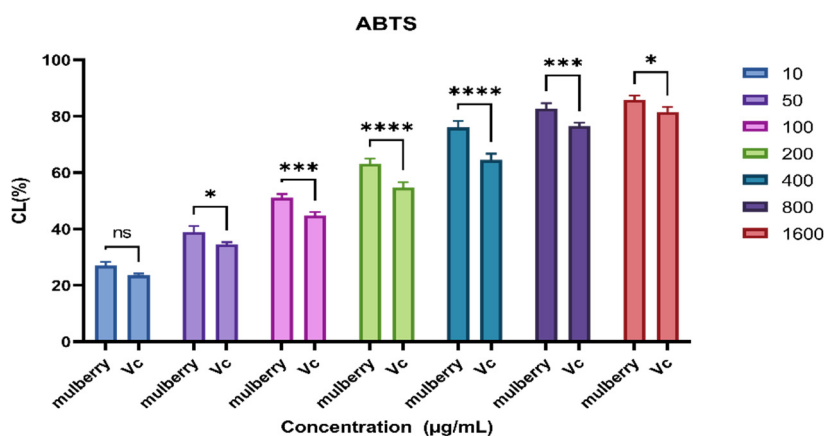


Figure 1. ABTS Free radical scavenging experiment

The results demonstrated that the mulberry extract exhibited significantly stronger antioxidant activity than vitamin C in both DPPH and ABTS assays ($p < 0.05$).

In the ABTS assay, the radical scavenging rate of the mulberry extract increased from $27.0 \pm 1.4\%$ to $85.9 \pm 1.4\%$ within the concentration range of 10–1600 $\mu\text{g/mL}$, consistently surpassing that of vitamin C at 23 $\mu\text{g/mL}$. Significant differences were observed at several concentrations: at 100 $\mu\text{g/mL}$ ($51.1 \pm 1.3\%$ vs. $44.8 \pm 1.2\%$, $p < 0.05$), as well as at 200 $\mu\text{g/mL}$ ($63.2 \pm 1.8\%$ vs. $54.7 \pm 1.9\%$) and 400 $\mu\text{g/mL}$ ($76.0 \pm 2.3\%$ vs. $64.5 \pm 2.0\%$).

Similarly, in the DPPH assay, the scavenging activity of the mulberry extract (ranging from $19.8 \pm 1.6\%$ to $84.8 \pm 2.1\%$) was significantly higher than that of vitamin C ($16.8 \pm 0.5\%$ to $80.6 \pm 1.7\%$) across tested concentrations. The difference was particularly notable at 400 $\mu\text{g/mL}$ (Figure 2).

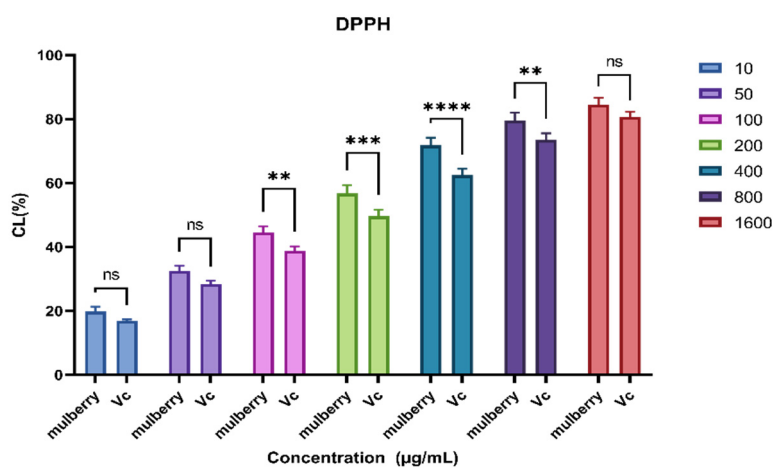


Figure 2. DPPH Free radical scavenging experiment

These findings indicate that the mulberry extract possesses strong, concentration-dependent antioxidant properties, which may contribute to its observed inhibitory effects on ferroptosis in HeLa cells.

3.2. Fe^{2+} and Fe^{3+} Ionic Chelating Ability of Mulberry Extracts

As shown in Figure 3, the extract demonstrated a remarkable concentration-dependent chelation activity toward both ionic forms ($p < 0.01$), with the chelation rate increasing progressively as the concentration rose. Experimental data revealed that at a concentration of 400 $\mu\text{g/mL}$, the chelation rate for Fe^{2+} reached $84.1 \pm 0.5\%$, significantly higher than that for Fe^{3+} ($74.8 \pm 0.4\%$; $p < 0.05$), suggesting a stronger affinity of the mulberry extract for Fe^{2+} .

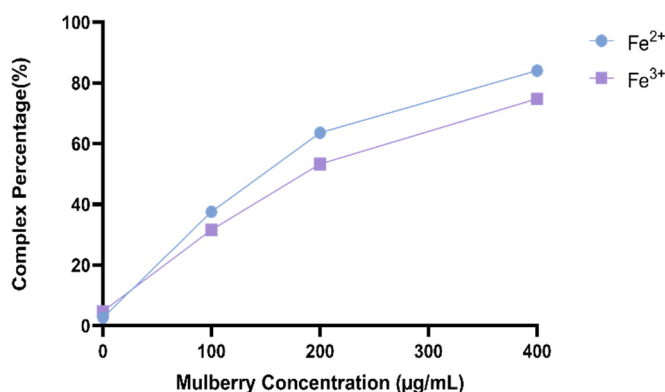


Figure 3. iron ion Chelating Agenteng ability

3.3. Effect of Mulberry Extract on Cell Proliferation

As shown in Figure 4, treatment with mulberry extract alone at various concentrations did not significantly affect the viability of HeLa cells. These results indicate that the mulberry extract exhibits no obvious cytotoxicity and does not promote the proliferation of cancer cells.

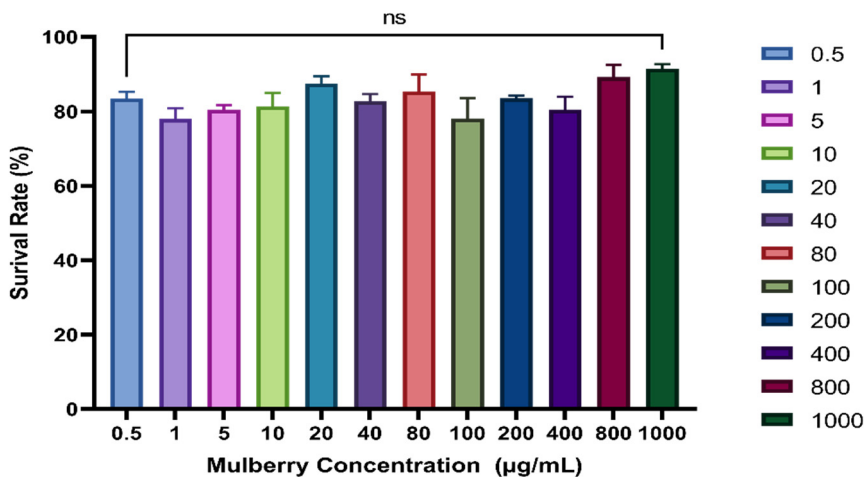


Figure 4. Mulberry cells were treated HeLa

3.4. Effect of Mulberry Extract on Ferroptosis

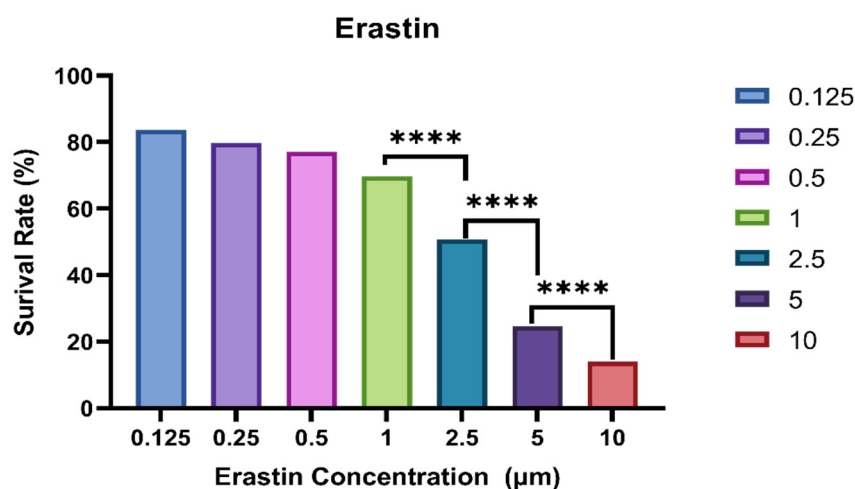


Figure 5. Erastin Process HeLa cells

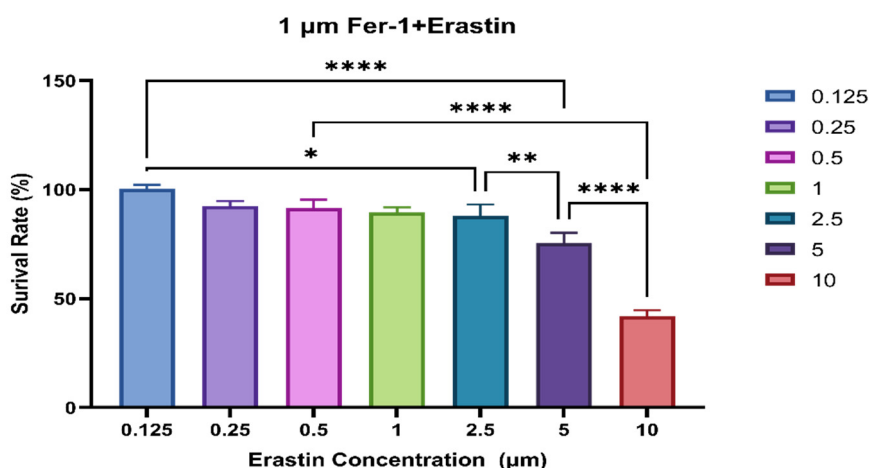


Figure 6. Fer-1 and Erastin were used to treat HeLa cells

MTT assay results demonstrated that mulberry extract significantly alleviated Erastin-induced ferroptosis in HeLa cells (Figure 5). Erastin treatment alone led to a concentration-dependent decrease in cell viability, reducing the survival rate to $50.71 \pm 0.7\%$ at $2.5 \mu\text{M}$ and to $13.96 \pm 0.4\%$ at $10 \mu\text{M}$, confirming its efficacy in inducing ferroptosis. To validate the experimental model, Ferrostatin-1 (Fer-1), a specific ferroptosis inhibitor, was co-administered with Erastin. The addition of Fer-1 markedly restored cell viability, maintaining survival rates above 88% at Erastin concentrations ranging from 0.125 to $2.5 \mu\text{M}$, thereby verifying the reliability of the ferroptosis induction system (Figure 6).

Based on prior results, three concentrations of mulberry extract (100 , 200 , and $400 \mu\text{g/mL}$) were selected to evaluate its protective effect against Erastin-induced toxicity. As shown in Figure 7 and Supplementary Figure 8, cells treated with mulberry extract exhibited significantly higher survival rates than those treated with Erastin alone, indicating that the extract antagonizes Erastin-induced ferroptosis in a dose-dependent manner.

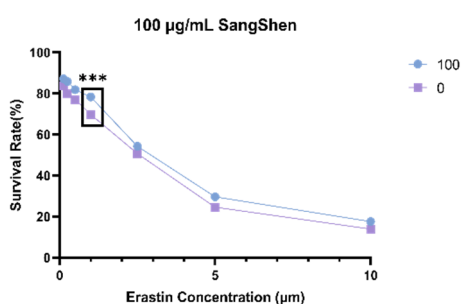


Figure 7. $100 \mu\text{g/mL}$ mulberry cells were treated with HeLa

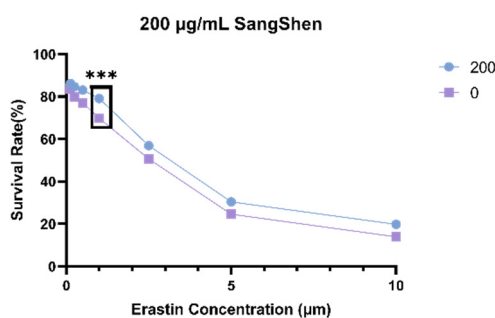


Figure 8. $200 \mu\text{g/mL}$ mulberry cells were treated with HeLa

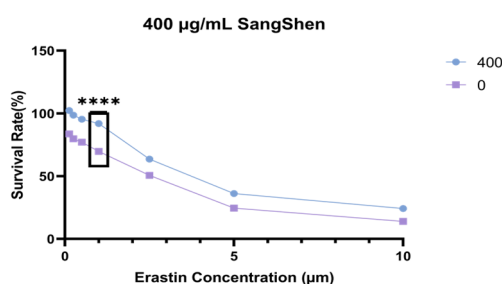


Figure 9. $400 \mu\text{g/mL}$ mulberry cells were treated with HeLa

In summary, mulberry extract effectively inhibits ferroptosis, with the most pronounced protective effect observed at $400 \mu\text{g/mL}$. These findings suggest that the complex composition of mulberry extract may include one or more components with Fer-1-like anti-ferroptotic activity.

3.5. Effect of Mulberry Extract on Intracellular Reduced GSH Content

Dynamic monitoring of glutathione (GSH) levels revealed that mulberry extract significantly counteracted Erastin-induced GSH depletion in HeLa cells (Figure 10). Treatment with $10 \mu\text{M}$

Erastin for 25 min reduced intracellular GSH content by $13.5 \pm 2.4\%$ compared to the blank control. Notably, mulberry extract alone did not significantly alter basal GSH levels, indicating that its action mechanism involves antagonizing Erastin-induced toxicity rather than directly promoting GSH synthesis.

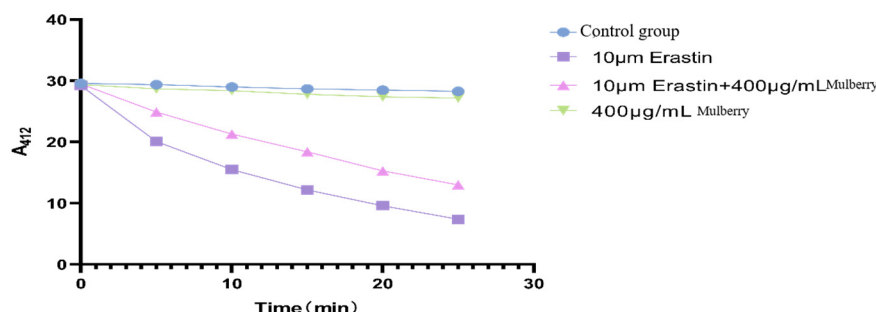


Figure 10. Effects of mulberry extract on GSH

3.6. Molecular Docking Analysis

Using molecular docking, we evaluated the binding affinity of 88 structurally characterized compounds from mulberry fruit against six key proteins involved in ferroptosis induction, including ALOX15 and ALOX12. The results are summarized in the heatmap shown in Figure 11.

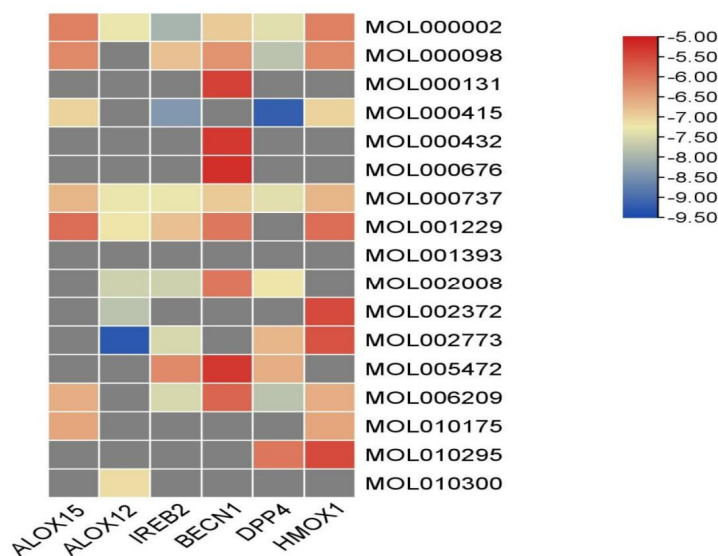


Figure 11. The docking ability of some compounds to six Ferroptosis driving proteins

Notably, the mulberry-derived compound MOL002773 exhibited a strong binding affinity to ALOX12. Further analysis identified myricetin and cis-resveratrol as potential competitive inhibitors targeting the active sites of BECN1 and DPP4, respectively (Figures 12, 13). These findings imply that mulberry extract may exert anti-ferroptotic effects via multi-target synergy, potentially involving ALOX12, BECN1, and DPP4.

4. Discussion

This study provides comprehensive evidence that mulberry fruit extract functions as a natural inhibitor of ferroptosis, employing an integrated mechanism that combines potent antioxidant activity, effective iron chelation, and multi-target regulatory potential.

Our initial chemical characterization confirmed that the extract possesses superior free radical scavenging capacity compared to vitamin C. More significantly, we demonstrated its

remarkable, concentration-dependent ability to chelate both Fe^{2+} and Fe^{3+} ions, with a distinct preference for Fe^{2+} . This specificity is critically important, as redox-active Fe^{2+} serves as the primary catalyst for the Fenton reaction, which drives the peroxidation of membrane phospholipids—the hallmark of ferroptosis [4]. Thus, the iron-chelating property of the extract likely constitutes a first line of defense, directly sequestering the catalytic core required for ferroptosis initiation.

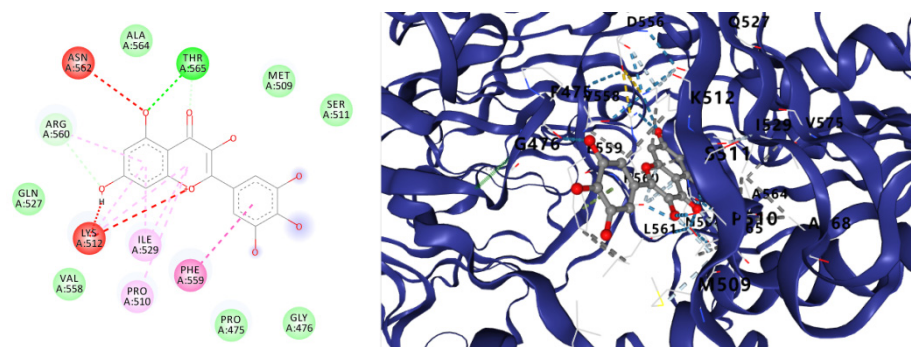


Figure 12. myricetin The docking results of BECN1 protein



Figure 13. Results of cis-resveratrol docking with DPP4 protein

In cellular models, the extract itself conferred significant protection against Erastin-induced ferroptosis. The restoration of cell viability and, more importantly, the mitigation of Erastin-induced GSH depletion are pivotal observations.

Molecular docking revealed that several bioactive compounds in mulberry, such as MOL002773, myricetin, and cis-resveratrol, can bind with high affinity to key ferroptosis regulators. The strong binding to ALOX12 suggests a direct mechanism to curb the generation of lethal lipid hydroperoxides [5]. BECN1 has been implicated in promoting ferroptosis by regulating system Xc- activity [18], while DPP4 inhibition is known to suppress lipid peroxidation. These in silico results propose a compelling "multi-target, multi-component" synergistic model, which is a hallmark of complex natural product extracts.

A pivotal finding of this study is that while the mulberry extract consistently demonstrated significant protection, its efficacy was quantitatively inferior to the synthetic, specific inhibitor Ferrostatin-1. This observed modest potency, rather than diminishing the significance of our work, provides a crucial insight into the bioactivity of complex natural extracts.

Therefore, the principal contribution of this research lies in the systematic mechanistic deconvolution of the anti-ferroptotic activity present in mulberry. This network-level intervention may offer advantages for managing complex disease states. Consequently, the next study is to move from the crude extract to the isolation and functional validation of individual constituents.

5. Conclusion

In conclusion, our integrated approach demonstrates that mulberry fruit extract effectively inhibits ferroptosis through a synergistic mechanism. This work not only elucidates a novel pharmacological activity of mulberry but also provides a solid experimental foundation for its development as a natural, multi-target agent against ferroptosis-related pathologies. Future research should focus on the isolation and functional validation of the primary active compounds, followed by an investigation of their efficacy in more complex physiological and disease models.

Acknowledgments

Natural Science Foundation.

References

- [1] Y. Liu, Y. Liu, D. Mu, et al. Preparation, structural characterization and bioactivities of polysaccharides from mulberry (*Mori Fructus*), *Food Biosci*, Vol. 46 (2022):101604.
- [2] S.J. Dixon, J.A. Olzmann. The cell biology of Ferroptosis, *Nature Reviews Molecular Cell Biol*, Vol. 25 (2024), No.6, p.424-442.
- [3] X. Jin, J. Tang, X. Qiu, X. Nie, et al. Ferroptosis: Emerging mechanisms, biological function, and therapeutic potential in cancer and inflammation, *Cell Death Discov*, Vol. 10 (2024), No.1, p.1-10.
- [4] Y. Kong, J. Li, R. Lin, et al. Understanding the unique mechanism of Ferroptosis: A promising therapeutic target, *Front Cell Dev Biol*, Vol. 11 (2024):1329147.
- [5] D.G. Liang, A.M. Minikes, X.J. Jiang. Ferroptosis at the intersection of lipid metabolism and cellular signaling, *Molecular cell*, Vol. 82 (2022), No.12, p.2215-2227.
- [6] S. Wang, Q. Guo, L. Zhou, X. Xia: Ferroptosis: A double-edged sword, *Cell Death Dis*, Vol. 10 (2024), No.1, p.1-16.
- [7] J. Wu, Y. Wang, R. Jiang, R. Xue, et al. Ferroptosis in liver disease: New insights into disease mechanisms, *Cell Death Dis*, Vol. 7 (2021), No.1, p.1-9.
- [8] X. Shan, J. Li, J. Liu, B. Feng, et al. Targeting Ferroptosis by poly(acrylic) acid coated Mn3O4 nanoparticles alleviates acute liver injury, *Nature Commun*, Vol. 14 (2023), No.1, p.1-15.
- [9] X.L. Yang, D. Yan. Function, mechanism of action, metabolism, and commercial application of *Lonicera japonica*: a review. *Food Science and Human Wellness*, p.1-37.
- [10] A. Floegel, D.O. Kim, S.J. Chung, et al. Comparison of ABTS/DPPH assays to measure antioxidant capacity in popular antioxidant-rich US Foods, *J Food Comp Anal*, Vol. 24 (2011), p.1043-1048.
- [11] S. Baliyan, R. Mukherjee, A. Priyadarshini, Determination of antioxidants by DPPH radical scavenging activity and quantitative phytochemical analysis of *Ficus religiosa*, *Molecules*, Vol. 27 (2022), No.4, p.1326.
- [12] W.W. Fish. Ferrozine---a new spectrophotometric reagent for iron, *Analytical Biochemistry*, Vol. 85 (1988), No.1, p.94-100.
- [13] P. Carter, Spectrophotometric determination of serum iron at the submicrogram level with a new reagent (ferrozine), *Analytical Biochemistry*, Vol. 40 (1971), No.2, p.450-458.

- [14] M.J. Hynes, Coinceanainn MÓ: The kinetics and mechanisms of the reaction of iron(III) with gallic acid, gallic acid methyl ester and catechin, *Journal of the Chemical Society*, Vol. 2 (2001), No.8, p.1526-1533.
- [15] Y. Fan, J. Chang, X. Qin, et al. Copper-Based Targeted Nanocatalytic Therapeutics for Non-Small Cell Lung Cancer, *Nano-Micro Letters*, Vol. 18 (2026), No.5, p.308-328.
- [16] D. Jin, J. Zhang, Y. Zhang, X. An, et al. Network pharmacology-based and molecular docking prediction of the active ingredients and mechanism of ZaoRenDiHuang capsules for application in insomnia treatment, *Comput Biol Med*, Vol. 135 (2021).104562
- [17] L. Fu, S. Shi, J. Yi. ADMETlab 3.0: an updated comprehensive online ADMET prediction platform enhanced with broader coverage, improved performance, API functionality and decision support, *Nucleic Acids Res*, Vol. 52 (2024), No. W1, p.W422-W431.
- [18] Y. Sun, Y. Zhuang, K. Cheng, et al. YTHDF2-orchestrated m6A methylation of BECN1 induces Scoparone-mediated hepatic stellate cell ferroptosis to attenuate liver fibrosis, *Phytomedicine: international journal of phytotherapy and phytopharmacology*, Vol. (2026).157912